DOI: 10.3901/CJME.2013.04.675, available online at www.springerlink.com; www.cjmenet.com; www.cjmenet.com.cn

Numerical Analysis on Nanoparticles-laden Gas Film Thrust Bearing

YANG Zhiru[1], DIAO Dongfeng[1, 2, *], and YANG Lei[1]

1 *Key Laboratory of Education Ministry for Modern Design and Rotor-Bearing System, Xi'an Jiaotong University, Xi'an 710049, China*

2 *Institute of Nanosurface Science and Engineering (INSE), Shenzhen University, Shenzhen 518060, China*

Received October 7, 2012; revised January 28, 2013; accepted March 22, 2013

Abstract: Nanoparticles can be taken as additives and added into various fluids to improve their lubricating performances. At present, researches in this area are mainly concentrated on the improvement effects of nanoparticles on the lubricating performances of liquid such as oil and water. Nanoparticles will also affect gas lubrication, but few related studies have been reported. Nanoparticles-laden gas film (NLGF) is formed when adding nanoparticles into gas bearing. Then, the lubricating performances of gas bearing including pressure distribution and load-carrying capacity will change. The variations of pressure distribution and load-carrying capacity in nanoparticles-laden gas film thrust bearing are investigated by numerical method. Taking account of the compressibility of gas and the interactions between gas and nanoparticles, a computational fluid dynamics model based on Navier-Stokes equations is applied to simulate the NLGF flow. The effects of inlet nanoparticles volume fraction and orifice radius on film pressure distribution and load-carrying capacity of the NLGF are calculated. The numerical calculation results show that both of the film land pressure and the maximum film pressure both increase when the nanoparticles are added into gas bearing, and the film pressures increase with the rising of the inlet nanoparticles volume fraction. The nanoparticles have an enhancement effect on load-carrying capacity of the studied bearing, and the enhancement effect becomes greater as the film thickness decrease. Therefore, nanoparticles can effectively improve the lubricating performance of gas bearing. The proposed research provides a theoretical basis for the design of new-type nanoparticles-laden gas film bearings.

Key words: load-carrying capacity, pressure distribution, nanoparticles-laden gas film, computational fluid dynamics

1 Introduction

Nanoparticles could be used as either lubricant[1] or lubricant additives[2]. As additives, nanoparticles was added in various fluids to improve their lubricating performances[3–4]. There were many studies on adding nanoparticles in lubricating oil[5–9]. RAPOPORT, et al[5], found that addition of even a small amount of nanoparticles into oil could increase its load-carrying capacity. LIU, et al[6], found that the oil exhibited excellent load-carrying capacity when the average size of the additive particles was less than 30 nm. HSIN, et al[7] and LIN, et al[8], both confirmed that nanoparticles of different material improved the load-carrying capacity of lubricating oil. LEE, et al[9], analyzed the mechanism of load-carrying capacity enhancement of nanoparticles on lubricating oil. The above-mentioned literatures are all about enhancement effects of nanoparticles on load-carrying capacity of lubricating oil.

When particles were added in gas, the pressure distribution of the mixture flow changed. Gas pressure in an orifice or nozzle outlet was significantly affected by particles concentration in a gas-particles mixture flow[10–16]. YUU, et al[10], reported that the presence of particles reduced the pressure drop by as much as 30% at the outlet. CHU, et al[11], found the pressure drop decreased with the increasing of particles concentration in a cyclone separator. WANG, et al[12–13] and LEE, et al[14], studied the aerodynamic focusing of nanoparticles, and provided numerical and experimental methods to investigate the gas-nanoparticles mixture flowing through a nozzle. MA, et al[15] and KIM, et al[16], studied pressure drop in gas-particles mixture flow using numerical and theoretical approach, respectively, and their model successfully predicted the mechanism of the pressure variation.

However, there are few studies discussing the effects of particles in gas-nanoparticles mixture which was applied as lubricant. In this study, in order to study the effects of inlet nanoparticles volume fraction and orifice radius on film pressure distribution, a nanoparticles-laden gas film (NLGF) formed by adding silica (SiO_2) nanoparticles into air bearing is simulated by computational fluid dynamics (CFD) method. Then, the film pressure distribution and load-carrying capacity in NLGF thrust bearing are

* Corresponding author. E-mail: dfdiao@mail.xjtu.edu.cn

This project is supported by National Natural Science Foundation of China (Grant No. 51175405)

calculated. Finally, the variation tendency of load-carrying capacity with nanoparticle volume fraction and film thickness is derived.

2 Numerical Analysis Method

2.1 Computational fluid dynamics model

Fig. 1 shows the geometrical configuration of the aerostatic NLGF thrust bearing with a single inlet port. The radius of the circular pad is 5 mm. An orifice restrictor with radius of 0.1–0.5 mm is located at the center of the pad. The nanoparticles-laden gas is consisted of air and uniformly dispersed silica nanoparticles (30 nm in diameter). The mixture flows through orifice, then enters the bearing clearance and flows out from the bearing edge at last. Because the flow field in the bearing is axisymmetric, the calculation can be simplified from three-dimensional (3D) to two-dimensional (2D), and the cross-section of the flow field (the shaded area in Fig. 1) is used for the 2D numerical simulation.

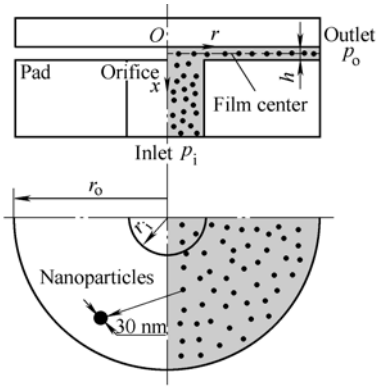

Fig. 1. Basic bearing model for numerical analysis

CFD method was widely used in the numerical analysis of gas film lubrication[17–18]. The Mixture Model was the common model to simulate the uniform two component flow[19]. In this model, the nanoparticles-laden gas mixture is treated as one fluid. The air and silica nanoparticles are considered as two components of the fluid, and the sum of their volume fractions is one. The compressibility of gas and the interactions between gas and nanoparticles are both considered in the flow. Therefore, the Navier-Stokes equations (include continuity equation and momentum equation), the volume fraction equation[20], the gas state equation and the energy conservation equation[21] are necessary for the analysis of the model.

In order to combine the interactions between gas and nanoparticles in the model, two items (F_x, F_r) are added in the momentum equations. Then, the momentum equations for the mixture in axial and radial direction can be expressed as follows:

$$\rho_{\mathrm{m}}\frac{\partial v_{\mathrm{m},x}}{\partial t}+\rho_{\mathrm{m}}v_{\mathrm{m},x}\frac{\partial v_{\mathrm{m},x}}{\partial x}+\rho_{\mathrm{m}}v_{\mathrm{m},r}\frac{\partial v_{\mathrm{m},x}}{\partial r}=-\frac{\partial p}{\partial x}+2\mu_{\mathrm{m}}\frac{\partial^2 v_{\mathrm{m},x}}{\partial x^2}+\frac{\mu_{\mathrm{m}}}{r}\frac{\partial}{\partial r}\left[r\left(\frac{\partial v_{\mathrm{m},x}}{\partial r}+\frac{\partial v_{\mathrm{m},r}}{\partial x}\right)\right]+\rho_{\mathrm{m}}g+F_x, \quad (1)$$

$$\rho_{\mathrm{m}}\frac{\partial v_{\mathrm{m},r}}{\partial t}+\rho_{\mathrm{m}}v_{\mathrm{m},x}\frac{\partial v_{\mathrm{m},r}}{\partial x}+\rho_{\mathrm{m}}v_{\mathrm{m},r}\frac{\partial v_{\mathrm{m},r}}{\partial r}=-\frac{\partial p}{\partial r}+\frac{\partial}{\partial x}\left[\mu_{\mathrm{m}}\left(\frac{\partial v_{\mathrm{m},r}}{\partial x}+\frac{\partial v_{\mathrm{m},x}}{\partial r}\right)\right]+2\mu_{\mathrm{m}}\left(\frac{1}{r}\frac{\partial v_{\mathrm{m},r}}{\partial r}+\frac{\partial^2 v_{\mathrm{m},r}}{\partial r^2}\right)-2\mu_{\mathrm{m}}\frac{v_{\mathrm{m},r}}{r^2}+F_r, \quad (2)$$

where ρ_{m} is the density of the mixture; $v_{\mathrm{m},x}$, $v_{\mathrm{m},r}$ are the velocities of the mixture in axial direction and radial direction, respectively; p is the pressure of the mixture; μ_{m} is the viscosity of the mixture; F_x, F_r are the drag forces of the mixture in axial direction and radial direction, respectively.

The drag force of the mixture in axial and radial direction can be expressed as follows:

$$F_x=\alpha_1\rho_1\left[\frac{\partial}{\partial x}(v_{\mathrm{dr1},x}v_{\mathrm{dr1},x})+\frac{1}{r}\frac{\partial}{\partial r}(rv_{\mathrm{dr1},r}v_{\mathrm{dr1},x})\right]+\alpha_2\rho_2\left[\frac{\partial}{\partial x}(v_{\mathrm{dr2},x}v_{\mathrm{dr2},x})+\frac{1}{r}\frac{\partial}{\partial r}(rv_{\mathrm{dr2},r}v_{\mathrm{dr2},x})\right], \quad (3)$$

$$F_r=\alpha_1\rho_1\left[\frac{\partial}{\partial x}(v_{\mathrm{dr1},x}v_{\mathrm{dr1},r})+\frac{1}{r}\frac{\partial}{\partial r}(rv_{\mathrm{dr1},r}v_{\mathrm{dr1},r})\right]+\alpha_2\rho_2\left[\frac{\partial}{\partial x}(v_{\mathrm{dr2},x}v_{\mathrm{dr2},r})+\frac{1}{r}\frac{\partial}{\partial r}(rv_{\mathrm{dr2},r}v_{\mathrm{dr2},r})\right], \quad (4)$$

where α_1, α_2 are the volume fractions of air and silica nanoparticles; ρ_1, ρ_2 are the densities of air and silica nanoparticles; $v_{\mathrm{dr1},x}$, $v_{\mathrm{dr2},x}$ are the drift velocity of air and silica nanoparticles in axial direction; $v_{\mathrm{dr1},r}$, $v_{\mathrm{dr2},r}$ are the drift velocity of air and silica nanoparticles in radial direction, respectively.

Based on the above mentioned equations, the film pressure distribution of the NLGF is obtained. The load-carrying capacity of NLGF is the integral of film pressure distribution, and it can be expressed as

$$W=\int_0^{r_o}2\pi rp(r)\mathrm{d}r, \quad (5)$$

where r_o is the pad radius and $p(r)$ is the film pressure distribution along film center in radial direction.

2.2 Calculation grids and boundary conditions

To solve the Navier-Stokes equations of the mixture, boundary conditions need to be defined and the fluid needs to be discretized to finite element grids. Fig. 2 shows the grids used in NLGF lubrication analysis. The flow field is divided into 2 500 elements in the axial direction and 1 010 in the radial direction. The element size is in the range from 0.29×10^{-12} m^2 to 4.1×10^{-12} m^2. In order to improve the accuracy of the calculation, the distance between grid points becomes smaller as the grid position is closer to the walls, as shown in the enlarged view of Fig. 2.

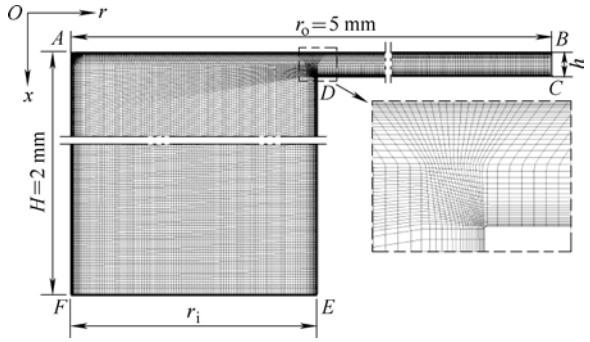

Fig. 2. Schematic view of grid for calculation of flow field

Boundary conditions are defined as follows.

Solid walls (edge *AB*, *CD*, and *DE*): The walls are considered to be impermeable and adiabatic. No-slip condition is set up at the walls, and the flow velocities in all directions at the walls are zero.

Symmetric axis (edge *AF*): At the central axis of the bearing, the density, the velocities and the energy are symmetric. The normal velocity component and the normal gradients for all variables at the axis are assumed zero.

Pressure inlet (edge *EF*): In the present simulation, the calculations are initiated from edge EF. The inlet pressure is 0.3 MPa and its direction is perpendicular to the inlet edge *EF*. The temperature at the inlet is 300 K.

Pressure outlet (edge *BC*): The outlet pressure is 0.1 MPa, which equals to ambient pressure, and its direction is perpendicular to the outlet edge *BC*. The temperature at the outlet is also 300 K.

A commercial code (FLUENT 6.3) was employed to establish the CFD model, as well as to calculate the film pressure distribution and load-carrying capacity of the NLGF. Firstly, the Mixture Model in FLUENT 6.3 was chosen to define the NLGF flow. SiO_2 nanoparticles were defined as the particle phase. The diameter, density and volume fraction of the nanoparticles were set. Secondly, energy equation was utilized, and ideal gas was defined as the gas phase. Thirdly, boundary conditions were set. Fourthly, the solution scheme was defined. The control volume-based technique was adopted to solve the flow governing equations. The heat transfer terms were centrally differenced, and the pressure terms were upwind differenced. Finally, iterations of the solution loop ended when the converged solution was obtained. All of the calculation parameters, including material properties of nanoparticles, structural parameters of bearing and boundary conditions, are summarized in Table 1.

3 Numerical Results Analysis and Discussion

In order to validate the CFD model, the numerical results of the CFD model with clean gas were compared with the former experimental results[22]. The normalized pressure of numerical results and experimental results are shown in Fig. 3, in which the conditions were film thickness h of 90 μm, orifice inlet pressure p_i of 0.4 MPa, orifice radius r_i of 1 mm and bearing radius r_o of 30 mm. It can be seen that the numerical results and the experimental results have the same variation tendency, and it coincides with Yoshimoto's numerical results[18]. Therefore, the CFD model can be used in NLGF flow field analysis.

Table 1. Calculation parameters

Calculation parameter		Value
Material property	Nanoparticles density ρ_2/(kg • m^{-3})	1 500
	Nanoparticles viscosity μ_2/(kg • s^{-1} • m^{-1})	0.001
	Inlet nanoparticles volume fraction α_2/%	0, 10, 20, 30, 40, 50, 60
Structural parameter	Film thickness h/μm	20, 30, 40, 50, 60
	Orifice radius r_i/mm	0.1, 0.2, 0.3, 0.4, 0.5
	Pad radius r_o/mm	5
Boundary parameter	Orifice inlet pressure p_i/MPa	0.3
	Ambient pressure p_o/MPa	0.1
	Temperature T/K	300

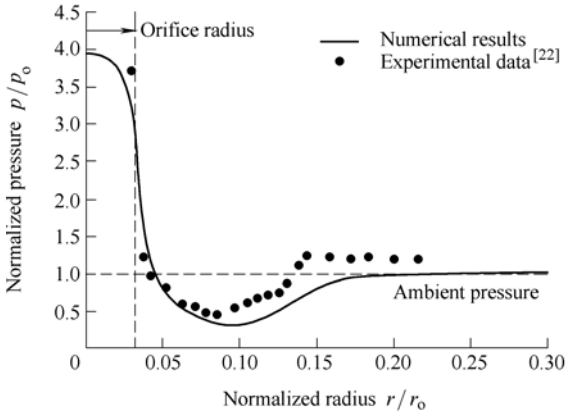

Fig. 3. Validation of numerical model

The pressure distribution along the film center ($h/2$) in radial direction was concerned in the study. Fig. 4 shows the effect of the inlet nanoparticles volume fraction on film pressure distribution under the conditions of h=20 μm, p_i=0.3 MPa, and r_i=0.4 mm.

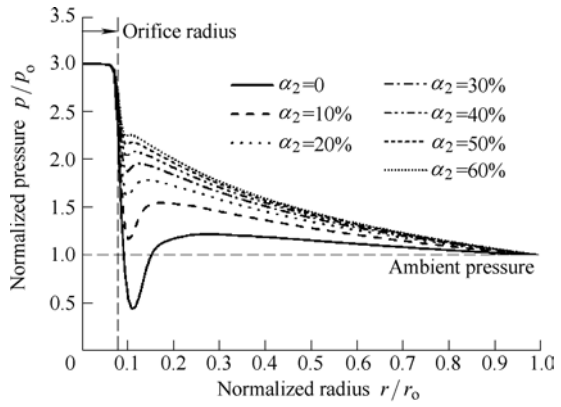

Fig. 4. Effect of the inlet nanoparticles volume fraction on film pressure distribution

The normalized pressure first showed a sudden drop near

orifice, then increased to maximum pressure and finally decreased slowly with the increasing of normalized radius along film center. The minimum pressure near orifice, named the film land pressure, affected the working stability of the NLGF; and the maximum pressure inside the film affected the load-carrying capacity of the NLGF. Therefore, the two pressures were concerned in the results analysis. It was clear that the film land pressure and maximum film pressure had the same variation trend, and both of them increased when the nanoparticles were added. In addition, as the inlet nanoparticles volume fraction (α_2) varied from 0 to 60%, the increment of film land pressure reduced and it was almost close to zero when the fraction was 60%.

Fig. 5 shows the film pressure distributions with different orifice radius when α_2 is 20%, h is 20 μm, and p_i is 0.3 MPa. It was found that the film land pressure increased as the orifice radius varied from 0.1 mm to 0.5 mm.

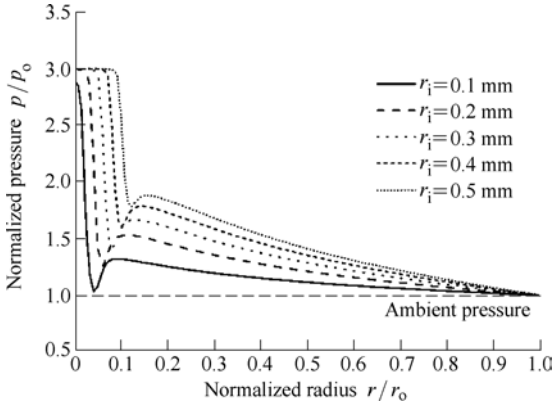

Fig. 5. Effect of the orifice radius on film pressure distribution

The load-carrying capacity was derived from film pressure distribution (see Eq. (5)). With the rising of film pressures, the load-carrying capacity increased. The increase ratio of load-carrying capacity was defined as the ratio of NLGF load-carrying capacity increment (W-W_0) to load-carrying capacity of gas film without nanoparticles (W_0). Fig. 6 shows the enhancement effects of inlet nanoparticles volume fraction on increase ratio of load-carrying capacity in various film thickness under the conditions of p_i=0.3 MPa and r_i=0.4 mm.

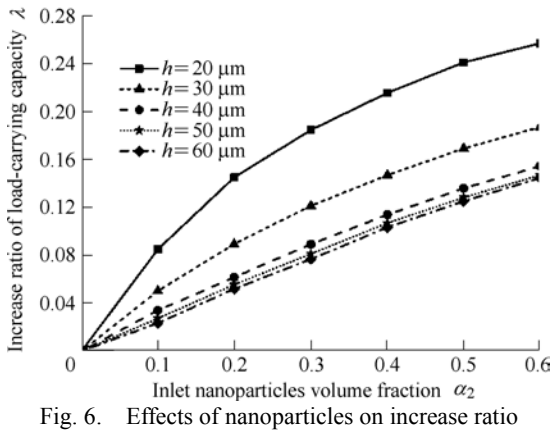

Fig. 6. Effects of nanoparticles on increase ratio of load-carrying capacity (LCC)

From Fig. 6, it was found that the load-carrying capacity increased with the increasing of inlet nanoparticles volume fraction. This was consistent with the results of film pressure distribution in Fig. 4. Moreover, the increase ratio of load-carrying capacity was greater in thin films than in thick films.

In this research, we found that the pressure and load-carrying capacity increased with the adding of nanoparticles. It was well known that the particles could uniformly disperse in air when the size was less than 10^{-7} m (100 nm)[23]. When they were added in a fluid, the viscosity of the fluid increased[21]. Thus, the pressure inside the film increased (pressure was proportional to viscous force), and then the load-carrying capacity (the integral of film pressure) increased. In addition, we also found that the load-carrying capacity increased with the increasing of nanoparticles volume fraction. This phenomenon was also caused by the increase of viscosity. When the nanoparticles volume fraction increased, the average distances between nanoparticles decreased and the interactions between them increased which caused the increase of the viscosity[24].

Due to the compressibility of gas, nanoparticles volume fraction inside the film is different with that at the inlet. The variation of nanoparticles volume fraction along film center was investigated under the conditions of h=20 μm, p_i=0.3 MPa, and r_i=0.4 mm. And the results are shown in Fig. 7. It can be seen that the nanoparticles volume fraction gradually decrease inside the film. However, the volume fractions of nanoparticles inside the film show the same trend of increasing as that of the inlet volume fraction. By this result, we can conclude that the increasing of inlet volume fraction increase the nanoparticles volume fraction inside the film, which contribute to higher load-carrying capacity. So it is reasonable to use inlet volume fraction to represent the state of the whole film, and nanoparticles volume fraction changing inside the film will not affect the conclusions.

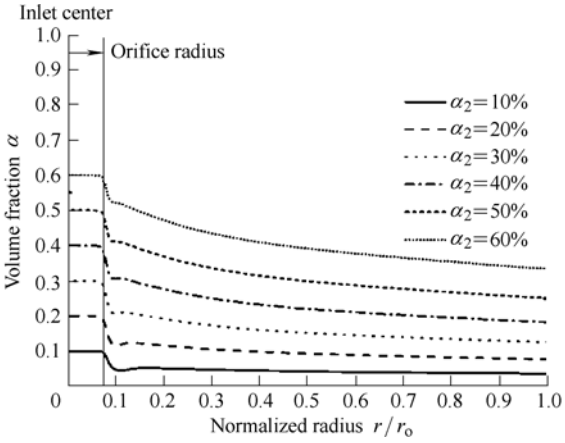

Fig. 7. The variation of nanoparticles volume fraction along film center (h/2)

4 Conclusions

(1) A CFD model of gas-nanoparticles two components

compressible flow is proposed to describe the flow field of nanoparticles-laden gas film thrust bearing.

(2) By adding nanoparticles into the gas film, the film land pressure and the maximum film pressure are both increased. The film pressures increase with the rising of the inlet nanoparticles volume fraction.

(3) The nanoparticles have an enhancement effect on load-carrying capacity of NLGF. The load-carrying capacity increases with the increasing of inlet nanoparticles volume fraction and the increase ratio of load-carrying capacity is greater in thin films than in thick films.

References

[1] TENNE R. Inorganic nanotubes and fullerene-like nanoparticles[J]. *Nature Nanotechnology*, 2006, 21(11): 103–111.

[2] LIU W M. Application of nanoparticles in lubricants[J]. *Tribology*, 2003, 23(4): 265–267. (in Chinese)

[3] ZHANG Y D, YAN J S, SUN L, et al. Friction reducing anti-wear and self-repairing properties of nano-cu additive in lubricating oil[J]. *Journal of Mechanical Engineering*, 2010, 46(5): 74–79. (in Chinese)

[4] FENG X J, LIU S J, CHAO Y. The effects of $MnZnFe_2O_4$ magnetic nanoparticles on thin film lubricating performance[J]. *Journal of Mechanical Engineering*, 2011, 47(7): 116–122. (in Chinese)

[5] RAPOPORT L, FLEISCHER N, TENNE R. Fullerene-like WS_2 nanoparticles: superior lubricants for harsh conditions[J]. *Advanced Materials*, 2003, 15(7–8): 651–655.

[6] LIU R D, WEI X C, TAO D H, et al. Study of preparation and tribological properties of rare earth nanoparticles in lubricating oil[J]. *Tribology International*, 2010, 43(5–6): 1 082–1 086.

[7] HSIN Y L, CHU H Y, JENG Y R, et al. In situ de-agglomeration and surface functionalization of detonation nanodiamond, with the polymer used as an additive in lubricant oil[J]. *Journal of Materials Chemistry*, 2011, 21(35): 13 213–13 222.

[8] LIN J S, WANG L W, CHEN G H. Modification of graphene platelets and their tribological properties as a lubricant additive[J]. *Tribology Letters*, 2011, 41(1): 209–215.

[9] LEE K, HWANG Y, CHEONG S, et al. Understanding the role of nanoparticles in nano-oil lubrication[J]. *Tribology Letters*, 2009, 35(2): 127–131.

[10] YUU S, JOTAKI T, TOMITA Y, et al. Reduction of pressure-drop due to dust loading in a conventional cyclone[J]. *Chemical Engineering Science*, 1978, 33(12): 1 573–1 580.

[11] CHU K W, WANG B, XU D L, et al. CFD-DEM simulation of the gas-solid flow in a cyclone separator[J]. *Chemical Engineering Science*, 2011, 66(5): 834–847.

[12] WANG X, KRUIS F, MCMURRY P H. Aerodynamic focusing of nanoparticles: I. guidelines for designing aerodynamic lenses for nanoparticles[J]. *Aerosol Science and Technology*, 2005, 39(7): 611–623.

[13] WANG X, GIDWANI A, GIRSHICK S L, et al. Aerodynamic focusing of nanoparticles: II. numerical simulation of particle motion through aerodynamic lenses[J]. *Aerosol Science and Technology*, 2005, 39(7): 624–636.

[14] LEE K S, KIM S, LEE D. Aerodynamic focusing of 5-50nm nanoparticles in air[J]. *Journal of Aerosol Science*, 2009, 40(12): 1 010–1 018.

[15] MA A C, WILLIAMS K C, ZHOU J M, et al. Numerical study on pressure prediction and its main influence factors in pneumatic conveyors[J]. *Chemical Engineering Science*, 2010, 65(23): 6 247–6 258.

[16] KIM S, LEE K B, LEE C G, et al. Theoretical approach for a pressure drop in two-phase particle-laden flows[J]. *International Communications in Heat and Mass Transfer*, 2007, 34(2): 153–161.

[17] LONG W, BAO G. Entrance effect on load capacity of orifice compensated aerostatic bearing with feeding pocket[J]. *Chinese Journal of Mechanical Engineering*, 2010, 23(4): 451–459.

[18] YOSHIMOTO S, YAMAMOTO M, TODA K. Numerical calculations of pressure distribution in the bearing clearance of circular aerostatic thrust bearings with a single air supply inlet[J]. *Journal of Tribology - Transactions of ASME*, 2007, 129(2): 384–390.

[19] MIETTINEN J, SCHMIDT H. CFD analyses for water-air flow with the Euler-Euler two-phase model in the FLUENT4 CFD code[C]//*Proceedings of the 10th International Conference on Nuclear Engineering*, Arlington, USA, April 14–18, 2002: ICONE10-22419.

[20] MANNINEN M, TAIVASSALO V, KALLIO S. *On the mixture model for multiphase flow*[M]. 1st ed. Espoo (Finland): VTT Publications, 1996.

[21] KOLEV N I. *Multiphase flow dynamics: fundamentals*[M]. 2nd ed. Berlin (Germany): Springer Press Ltd., 2007.

[22] MORI H, EZUKA H. A Pseudo Shock theory of pressure depression in externally pressurized circular thrust gas bearings[C]//*Proceedings of the JSLE-ASLE International Lubrication Conference*, Tokyo, Japan, June 9–11, 1975: 286–292.

[23] VINCENT J H, *Aerosol science for industrial hygienists*[M]. 1st ed. New York: Elsevier Science Inc., 1995.

[24] KOMODA Y, NAKASHIMA K, HIROSHI H, et al. Viscosity measuring technique for gas-solid suspensions[J]. *Advanced Powder Technology*, 2006, 17(3): 333–343.

Biographical notes

YANG Zhiru, born in 1981, is currently a PhD candidate at *Key Laboratory of Education Ministry for Modern Design and Rotor-Bearing System, Xi'an Jiaotong University, China*, in 2008. His research interests include gas-particles two phase lubrication and fluid film bearing.
Tel: +86-29-82669151; E-mail: yangzhiru2020@126.com

DIAO Dongfeng, born in 1961, is currently a professor, a PhD candidate supervisor and the director of *Key Laboratory of Education Ministry for Modern Design and Rotor-Bearing System, Xi'an Jiaotong University, China*. His main research interests include nano-scale and micro-scale particles environment tribology, nano-tribology and surface sciences.
Tel: +86-29-82669151; E-mail: dfdiao@mail.xjtu.edu.cn

YANG Lei, born in 1987, is currently a PhD candidate at *Key Laboratory of Education Ministry for Modern Design and Rotor-Bearing System, Xi'an Jiaotong University, China*, in 2010. His research interests include nano-scale wear and lubrication, nano-surface engineering.
Tel: +86-29-82669151; E-mail: yolai1015@stu.xjtu.edu.cn